Development 138, 4523-4533 (2011) doi:10.1242/dev.070706
© 2011. Published by The Company of Biologists Ltd

Alpha sarcoglycan is required for FGF-dependent myogenic progenitor cell proliferation in vitro and in vivo

Marco Cassano[1], Arianna Dellavalle[2], Francesco Saverio Tedesco[2], Mattia Quattrocelli[1], Stefania Crippa[1], Flavio Ronzoni[3], Agnese Salvade[4], Emanuele Berardi[1], Yvan Torrente[5], Giulio Cossu[2,6] and Maurilio Sampaolesi[1,3,*]

SUMMARY

Mice deficient in α-sarcoglycan (*Sgca*-null mice) develop progressive muscular dystrophy and serve as a model for human limb girdle muscular dystrophy type 2D. *Sgca*-null mice suffer a more severe myopathy than that of *mdx* mice, the model for Duchenne muscular dystrophy. This is the opposite of what is observed in humans and the reason for this is unknown. In an attempt to understand the cellular basis of this severe muscular dystrophy, we isolated clonal populations of myogenic progenitor cells (MPCs), the resident postnatal muscle progenitors of dystrophic and wild-type mice. MPCs from *Sgca*-null mice generated much smaller clones than MPCs from wild-type or *mdx* dystrophic mice. Impaired proliferation of *Sgca*-null myogenic precursors was confirmed by single fiber analysis and this difference correlated with *Sgca* expression during MPC proliferation. In the absence of dystrophin and associated proteins, which are only expressed after differentiation, SGCA complexes with and stabilizes FGFR1. Deficiency of *Sgca* leads to an absence of FGFR1 expression at the membrane and impaired MPC proliferation in response to bFGF. The low proliferation rate of *Sgca*-null MPCs was rescued by transduction with *Sgca*-expressing lentiviral vectors. When transplanted into dystrophic muscle, *Sgca*-null MPCs exhibited reduced engraftment. The reduced proliferative ability of *Sgca*-null MPCs explains, at least in part, the severity of this muscular dystrophy and also why wild-type donor progenitor cells engraft efficiently and consequently ameliorate disease.

KEY WORDS: Myogenic progenitor cells, Limb girdle muscular dystrophy, Cell therapy, Mouse

INTRODUCTION

Sarcoglycans are dystrophin-associated proteins (DAPs) that form a membrane complex necessary for the physiological function of skeletal and cardiac muscles (Henry and Campbell, 1996; Lapidos et al., 2004). Mutations in genes encoding sarcoglycans produce muscular dystrophy and cardiomyopathy in animal models and humans (Vainzof et al., 1996). Mice null for α-sarcoglycan (*Sgca*-null mice) (Duclos et al., 1998), a model for human limb girdle type 2D muscular dystrophy (LGMD2D), develop a more severe myopathy than *mdx* mice (Lefaucheur et al., 1995; McArdle et al., 1995), the standard model for Duchenne muscular dystrophy (DMD). In humans however, DMD is more severe than LGMD2D (McNally et al., 1994) and the reason for this discrepancy is unknown. Similarly, why the *mdx* mouse develops a relatively mild myopathy compared with human DMD is unknown. However, it has been proposed that there is a more robust self-renewal of myogenic progenitor cells (MPCs) in murine DMD as compared with the human disease (Blau et al., 1983). This has been demonstrated in telomerase knockout *mdx* mice, which exhibit premature exhaustion of the MPC pool and a more severe disease phenotype (Sacco et al., 2010). These mice more closely represent the human DMD phenotype, highlighting the role of MPC self-renewal in DMD severity.

MPCs are a population of muscle progenitors that are able to exit quiescence, proliferate and differentiate into new muscle fibers in response to muscle damage. They also play a key role in muscle regeneration (Alameddine et al., 1989; Le Grand and Rudnicki, 2007; Mauro, 1961; Shinin et al., 2006; Zammit et al., 2004; Zammit et al., 2006). We observed that MPCs from *Sgca*-null mice have a reduced proliferative ability in comparison to MPCs from wild-type or *mdx* dystrophic mice. This is due to a molecular interaction between SGCA and fibroblast growth factor receptor 1 (FGFR1) during the proliferative phase. We propose that SGCA modulates FGFR1 activity via the formation of a complex, and that the absence of SGCA destabilizes FGFR1, leading to the proliferative impairment of MPCs. This phenomenon, together with the enhanced apoptosis previously reported (Allikian et al., 2004; Anastasi et al., 2004; Yoshida et al., 1998), might explain the severity of this form of muscular dystrophy in mice and the success of previous cell transplantation experiments (Sampaolesi et al., 2003).

MATERIALS AND METHODS

Reagents

A monoclonal antibody (mAb) against SGCA was purchased from Novocastra (Newcastle, UK) and Kevin Campbell (Iowa University, USA) kindly provided an SGCA polyclonal antibody. Biotinylated rat mAb anti-SM/C2.6 was kindly provided by So-ichiro Fukada (Osaka University, Japan). Mouse monoclonal myogenin, MF20 and PAX7 antibodies were purchased from the Developmental Studies Hybridoma Bank. Mouse mAb against β-tubulin, rabbit polyclonal antibody (pAb) against MYOD and MYF5 were from Santa Cruz (San Diego, CA, USA). Mouse mAb anti-FGFR1 (#05-149, clone 19B2), rabbit pAb anti-FGFR4 and pHH3 antibodies were purchased from Chemicon (Millipore, Billerica, MA,

[1]Laboratory of Translational Cardiomyology, Stem Cell Interdepartmental Institute, KU Leuven, Herestraat 49 O&N1 bus 814, 3000 Leuven, Belgium. [2]Division of Regenerative Medicine, San Raffaele Scientific Institute, Via Olgettina 58, 20132 Milan, Italy. [3]Human Anatomy, University of Pavia, Via Forlanini 8, 27100 Pavia, Italy. [4]Laboratory of Cell Therapy 'Stefano Verri' University of Milan-Bicocca, 20052 Monza, Italy. [5]Stem Cell Laboratory, Department of Neurological Science, Fondazione IRCCS Cà Granda Ospedale Maggiore Policlinico, Centro Dino Ferrari, University of Milan, 20122 Milan, Italy. [6]Department of Biology, University of Milan, Via Celoria 28, 20129 Milan, Italy.

*Author for correspondence (maurilio.sampaolesi@med.kuleuven.be)

Accepted 11 August 2011

USA). Phospho-p44/42 MAPK (Thr202/Tyr204) rabbit mAb and p44/42 MAPK rabbit mAb were from Cell Signaling (Danvers, MA, USA). mAbs anti-β-galactosidase, V5 and GFP were purchased from Invitrogen (Carlsbad, CA, USA). Rabbit mAb anti-CycD, mouse mAb anti-GAPDH and rabbit pAb anti-syndecan 1 were provided by Abcam (Cambridge, MA, USA). Alexa Fluor secondary antibodies were purchased from Molecular Probes (Invitrogen).

Apoptosis was also evaluated by immunohistochemistry using a TUNEL assay (BioVision). Cytokine treatments were prepared by adding 5 ng/ml recombinant murine HGF (eBiosciences, San Diego, CA, USA) or bFGF (Peprotech, Rocky Hill, NJ, USA) to cell culture media. Human bFGF (5 ng/ml) and human recombinant HGF (5 ng/ml) were from Invitrogen. YP-740 was from Biotrend Chemikalien (Köln, Germany) and phorbol 12-myristate 13-acetate (PMA) was from Sigma-Aldrich (St Louis, MO, USA). Nuclei were always counterstained with DAPI (Invitrogen).

Plasmid cloning and expansion

Plasmids were prepared using standard procedures. All plasmid preparations were obtained using a GenElute HP Endotoxin-Free Plasmid Maxiprep Kit (Sigma-Aldrich) and quantified using a Nanodrop ND-1000 spectrophotometer. pCMV-SPORT6 plasmids carrying murine *Fgfr1* or *Sgca* cDNAs were purchased from Open Biosystems (Thermo Scientific, Huntsville, AL, USA).

RNA isolation and PCR analysis

Total RNA from MPCs was extracted using the PureLink RNA Mini Kit (Invitrogen) and genomic DNA was removed using the TURBO DNA-Free Kit (Ambion). Muscle extracts were homogenized in Trizol (Invitrogen) before proceeding to column purification. RNA was quantified and then reverse transcribed using the Superscript III Reverse Transcriptase Kit (Invitrogen). For PCR analysis we used Platinum Taq DNA polymerase (Invitrogen). For quantitative (q) PCR analysis, Fast SYBR Green Master Mix (Invitrogen) was diluted with cDNA and primers. RT-PCR and qPCR were performed using the following primers (Fw, forward; Rv, reverse; 5′ to 3′):

Sgca, Fw TCTGTCACTCACCGGGCGG and Rv GTGACCTCAATG-ACCTGGAG;

Gapdh, Fw TTCACCACCATGGAGAAGGC and Rv GGCATGGA-CTGTGGTCATGA;

Fgfr1, Fw ACAAACCCAACCGTGTGACCAAAG and Rv TTGG-AGGCGTACTCCACAATGACA; and

Fgfr4, Fw AGCCTGGTGATGGAAAGTGTGGTA and Rv ACACCTTG-CAGAGTAGCTCCACAT.

MPC isolation

MPCs were prepared as described (Cossu et al., 1980). Briefly, CD1 mice were sacrificed by cervical dislocation and the hindlimb muscles were removed. Muscle fragments were digested with 2% collagenase II (Invitrogen) for 60 minutes at 37°C. Digested cells were discarded and fragments were incubated again with 0.05% trypsin for 15 minutes at 37°C with gentle agitation. After the incubation, isolated cells were collected and fragments were incubated again until the whole tissue was digested. Isolated cells were pooled, centrifuged and resuspended in DMEM supplemented with 20% pre-screened fetal bovine serum (FBS), 5% horse serum (HS), 5% chicken embryo extract (CEE), 1% gentamycin, and then plated onto collagen-coated dishes at 10^4 cells/cm^2. Cells were pre-plated on plastic dishes for 3 hours in order to reduce contamination by non-myogenic cells.

For FACS-based sorting methods, cells from tissue extracts were counted and incubated with biotin-conjugated anti-SM/C2.6, anti-CD45-FITC and anti-CD31-PE for 1 hour at room temperature (RT). A second incubation step with streptavidin-APC was performed for 1 hour at RT. SM/C2.6$^+$/CD45$^-$/CD31$^-$ MPCs were sorted by flow cytometry (BD FACSDiva option).

Human myoblast derivation and culture

Healthy human myoblasts were prepared from the skeletal muscle tissue of a 30-year-old patient undergoing post-traumatic surgery (all patients signed a specific informed consent approved by the institutional Ethics Committee at San Raffaele Hospital, Milan, Italy) and were maintained in culture as previously described (Dellavalle et al., 2007). Additionally, cells were FACS screened for the myoblast marker CD56 (NCAM1) (Miltenyi Biotec, 130-090-755) to confirm their phenotype. LGMD2D myoblasts were obtained from a biopsy sample (32-year-old patient) kindly provided by the Telethon Genetic BioBank Network, specifically by Dr Maurizio Moggio (Director, Bank of DNA, Cell Lines and Nerve-Muscle-Cardiac Tissues, Ospedale Maggiore Policlinico Mangiagalli e Regina Elena, Milan, Italy).

Cell culture

Mouse myogenic cell line C2C12, human myoblasts and the 293T cell line were maintained in DMEM with 10% FBS. C2C12 and MPCs were induced to differentiate into myotubes by replacing 10% FBS with 2% HS. Differentiation was completed in 5 days. For MAPK stimulation experiments, proliferating *Sgca*-null MPCs were stimulated for 30 minutes at 37°C with YP-740 (10 μM) or PMA (100 ng/ml).

Single fiber isolation

Extensor digitorum longus (EDL) and soleus muscles from adult C57BL10 mice were isolated and digested in 0.008% collagenase type I (Sigma-Aldrich) for 20 minutes. Bundles of fibers protruding from the muscles were then collected using a wide-mouth glass Pasteur pipette. Following serial dilutions, single fibers were plated in 24-well plates coated with Matrigel (BD Biosciences). At day 1, plating medium was switched to proliferation medium (DMEM with 20% FBS, 1% CEE and 1% Pen/Strep) to allow proliferation of myogenic precursors. At day 5, myogenic precursors were fixed and stained for PAX7 and MYF5.

Western blotting

Cell pellets or tissue extracts were suspended in lysis buffer (RIPA buffer, pH 7.5; Sigma-Aldrich) supplemented with a Protease Inhibitor Cocktail (Roche). The whole-cell lysate or tissue extract was then centrifuged at 17,000 ***g*** for 10 minutes at 4°C. Protein lysates were boiled in SDS sample buffer for 5 minutes, subjected to 10% SDS-PAGE under reducing conditions and transferred onto Immobilon-P membranes (Millipore) using a semi-dry blotting apparatus (BioRad). The membranes were blocked with TBS-T buffer (Tris-buffered saline with 0.1% Tween 20) containing 5% skimmed milk for 30 minutes at RT and then incubated in TBS-T containing 5% skimmed milk with primary antibodies. The membranes were washed with TBS-T and incubated with horseradish peroxidase (HRP)-conjugated secondary antibody. Protein bands were detected using an enhanced chemiluminescence substrate (Amersham Biosciences) and a Fuji scanner equipped with a CCD camera.

Transfection assays

Transfection experiments were carried out using Lipofectamine 2000 (Invitrogen). The day before transfection, cells were seeded according to the manufacturer's protocol. On day 0, DNA-Lipofectamine complexes were incubated for 20 minutes at RT, added directly to the cell lines and left overnight. The following day, transfection medium was removed and replaced with proliferation medium.

Caspase 9 enzyme-linked immunosorbent assay (ELISA)

Active caspase 9 (Casp9) levels were measured using a mouse Caspase 9 ELISA Kit (#CSB-E08864m, Hoezel Diagnostika, Germany). Wild-type and *Sgca*-null MPCs cultured for 3 days in low-serum media with or without bFGF and HGF were processed to obtain cell lysates. Protein extracts were diluted to obtain equal starting concentrations and incubated in 96-well plates pretreated with anti-active Casp9 antibody. The total amount of active Casp9 was quantified using a Casp9-biotin/streptavidin-HRP conjugating system and measured using an ELISA reader at 450 nm.

Biotinylation of surface proteins

Surface protein biotinylation was performed using the Cell Surface Protein Isolation Kit (#89881, Pierce). Briefly, four T75 flasks containing ~1×10^6 wild-type or *Sgca*-null MPCs were used as starting material and treated for 2 hours at 4°C with sulfo-NHS-SS-biotin. Biotin-labeled surface proteins were incubated for 2 hours with NeutrAvidin Agarose resin columns. Finally, surface proteins were eluted and subject to western blot analysis.

Immunoprecipitation assays

Fifty microliters of Dynabeads Protein G (#10007D, Invitrogen) were incubated for 1 hour at RT with 1.5 mg rabbit polyclonal anti-SGCA antibody to allow antibody coupling. Protein extracts (1-4 mg) were incubated overnight at 4°C with the antibody-coupled magnetic beads. As a negative control, parallel incubations with an irrelevant antibody were performed. The immune complexes were washed five times, eluted in 20 µl elution buffer and then incubated with 20 µl 2× Laemmli buffer at 70°C for 5 minutes. Immunoprecipitated complexes were detected with FGFR1 and SGCA antibodies.

Lentiviral transduction of MPCs

MPCs were transduced as described (Sampaolesi et al., 2003) with pLenti6-V5/*Sgca* or with lentiviral vector pLenti-CMV/NLS-nlacZ. pGIPZ-shFgfr1 and pGIPZ-shScramble vectors were purchased from Open Biosystems. Following infection, transduced cells were selected in media containing puromycin (5 µg/ml).

Immunostaining

Primary cultures of MPCs were washed with PBS and fixed with 4% paraformaldehyde (PFA) for 10 minutes at 4°C. Cells were stained with primary antibodies overnight at 4°C and then incubated with species-specific secondary antibodies for 40 minutes at RT. For tissue histology, serial muscle sections were fixed with 4% PFA, permeabilized with 0.2% Triton X-100, rinsed with 1% BSA in PBS and then immunostained with β-galactosidase antibody.

Microscopy and image acquisition

Phase contrast images were taken with a Nikon ECLIPSE TS-100 microscope. Immunofluorescence staining analysis was performed using a Nikon ECLIPSE Ti-S inverted microscope. Image editing was performed using ImagePro software (Media Cybernetics). Confocal images were taken with a Leica TCS SPE.

Statistical analysis

Values are expressed as mean ± s.e.m. When two groups were compared, an unpaired Student's *t*-test was used. $P<0.05$ was considered statistically significant. When three groups were compared, and a two-way ANOVA was used, $P<0.05$ was also considered statistically significant (Bonferroni post-hoc test). The statistical significance of the differences between percentage values was assessed using a Kruskal-Wallis one-way analysis of variance by ranks test. α represents the significance in each independent case.

RESULTS

MPC isolation and morphological characterization

We analyzed the clonogenic ability of MPCs isolated from the soleus and tibialis anterior muscles of wild-type (wt), *Sgca*-null and *mdx* mice (Fig. 1A). The total number of MPC clones per muscle was increased for *Sgca*-null mice, but the total number of cells per single clone was dramatically reduced (Fig. 1B,C). We hypothesized that the increased number of MPC clones could be due to continuous

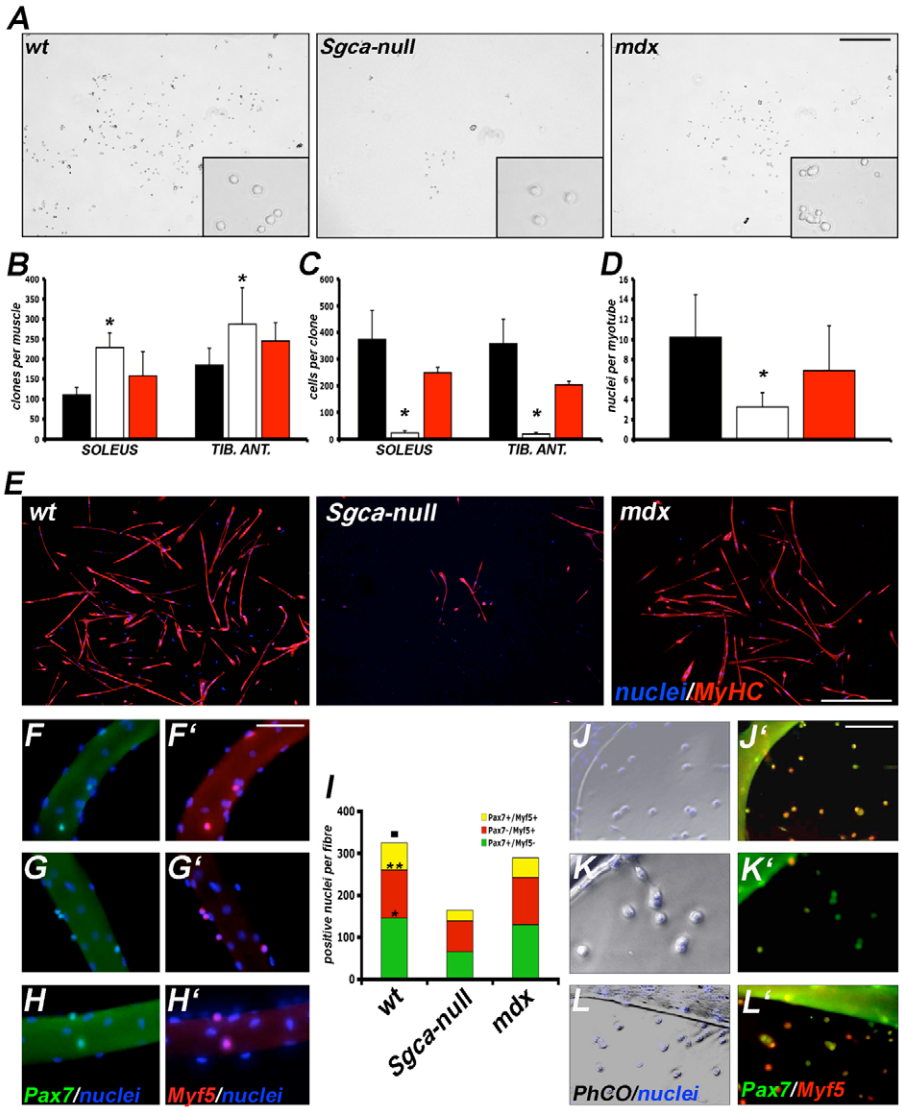

Fig. 1. Clonal and proliferative analyses of wild-type and *Sgca*-null myogenic progenitor cells. (**A**) Myogenic progenitor cells (MPCs) from the soleus and tibialis anterior muscles of 3-month-old wild-type (wt), *Sgca*-null and *mdx* mice. Insets show MPCs at higher magnification. $n=3$. (**B**) Total number of MPC clones from *Sgca*-null (white), wt (black) and *mdx* (red) mice. $n=100$; *, $P<0.01$ for *Sgca* null versus wt. (**C**) Total number of cells from single clones of *Sgca*-null (white), wt (black) and *mdx* (red) MPCs. $n=100$; *, $P<0.01$ for *Sgca* null versus wt. (**D**) Mean number of nuclei per myotube in wt (black), *Sgca*-null (white) and *mdx* (red) MPCs at day 5 of differentiation. $n=100$; *, $P<0.01$ for *Sgca* null versus wt. Error bars (B-D) indicate s.e.m. (**E**) MyHC staining of differentiated MPCs from wt, *Sgca*-null and *mdx* mice. $n=3$. (**F-H'**) Isolated myofibers from EDL and tibialis anterior muscles of 8-week-old wt (F,F'), *Sgca*-null (G,G') and *mdx* (H,H') mice fixed at time of isolation and stained for PAX7 (green in F,G,H) or MYF5 (red in F',G',H'). $n=5$. (**I**) Total number of MPCs per single fiber at day 5 following isolation. $n=5$; *, $P<0.01$ for $PAX7^+/MYF5^-$ *Sgca* null versus wt; **, $P<0.05$ for $PAX7^-/MYF5^+$ *Sgca* null versus wt; square, $P<0.05$ for $PAX7^+/MYF5^+$ *Sgca* null versus wt. (**J-L'**) Representative images from EDL and tibialis anterior isolated myofibers associated with their MPC progeny following 5 days of culture in proliferation medium. Isolated myofibers were obtained from 8-week-old wt (J,J'), *Sgca*-null (K,K') and *mdx* (L,L') mice and immunostained for PAX7 (green) and MYF5 (red) as satellite cell markers. Scale bars: 100 µm in A,E; 50 µm in F-H',J-L'.

regeneration attempts in dystrophic mice that might augment the percentage of activated MPCs. This feature is indeed common to the *mdx* mouse (Fukada et al., 2010). However, the increased clone number does not compensate for the smaller clone size as the overall number of MPCs obtained per single isolation was strongly reduced in *Sgca*-null compared with both wt and *mdx* mice (see Fig. S1A in the supplementary material). However, *mdx*-isolated MPCs had approximately the same number of cells per clone as wt.

The number of nuclei per myotube was consistently reduced in *Sgca*-null clones compared with both wt and *mdx* clones (Fig. 1D). After 5 days in differentiation medium, anti-myosin heavy chain (MyHC) immunostaining revealed large MyHC^{+} myotubes in both wt and *mdx* clones but only a few, thin myotubes in *Sgca*-null clones (Fig. 1E), as a consequence of the reduced MPC number.

The contamination rate of non-myogenic cells in our MPC clonal cultures was extremely low (wt, 2.75±0.65; *Sgca* null, 3.45±0.97; percentage of non-myogenic cells ± s.e.m.) and comparable to a FACS-based isolation method (wt, 1.23±0.33; *Sgca* null, 2.867±0.96), excluding the possibility that the biological differences observed could be attributed to a significant presence of non-myogenic cells (see Fig. S1B-F in the supplementary material).

The proliferation defect of *Sgca*-null myogenic precursors was further confirmed by single fiber analysis (Fig. 1F-L). At early time points, *Sgca*-null and *mdx* mice showed a small increase in the total number of PAX7^{+} satellite cells per fiber compared with the wt counterpart, confirming the results obtained from clonal MPCs (Fig. 1F-H; statistical analysis not shown). After 5 days in proliferation medium, the total number of satellite cell-derived MPCs was dramatically decreased for *Sgca*-null-derived myofibers compared with wt and *mdx* MPCs (Fig. 1I-L). However, the proportion of cells in the different compartments (PAX7^{+}/MYF5^{-}, PAX7^{+}/MYF5^{+} and PAX7^{-}/MYF5^{+}) did not appear to be drastically altered (Fig. 1I, red, green and yellow bars) when compared with wt and *mdx* counterparts.

Timecourse of *Sgca* expression in MPCs

Sgca is known to be expressed together with other dystrophin-glycoprotein complex (DGC)-associated components in differentiated myofibers, but not during proliferation, at least in the C2C12 myogenic cell line in which it has been investigated (Liu and Engvall, 1999). We examined *Sgca* expression during the proliferation and differentiation of wt MPCs. As expected, C2C12 cells did not express SGCA during proliferation (Fig. 2A, lane pC2C12), whereas expression was observed in proliferating MPCs at an early stage and this increased during differentiation (Fig. 2B and see Fig. S2A in the supplementary material). Differentiation endpoints corresponded to the highest expression level of SGCA (Fig. 2A,B), when the protein assumes its structural role as a member of the DGC complex (Lapidos et al., 2004). Interestingly, we observed that some as yet undifferentiated wt MPCs expressed SGCA before myogenin (Fig. 2C), while many cells co-expressed both proteins (Fig. 2C‴, yellow arrows). Moreover, several PAX7^{+} wt MPCs, corresponding to self-renewing cells, were found to be positive for SGCA expression (Fig. 2D‴, yellow arrows); for quantification of the PAX7^{+}/SGCA^{+} pool (54.67±2.34%) from freshly isolated wt MPCs, see Fig. S2B in the supplementary material.

HGF and bFGF effects on wt and dystrophic MPCs

Cytokine treatment is known to enhance MPC proliferation (Allen and Boxhorn, 1989). We tested the effect of two potent mitogenic cytokines – hepatocyte growth factor (HGF) and basic fibroblast growth factor (bFGF; also known as FGF2) – on wt and dystrophic MPCs. As already reported, bFGF stimulates robust wt and *mdx* MPC proliferation in vitro (Fig. 3A, gray lines) (DiMario and Strohman, 1988; Johnson and Allen, 1995; Smith and Schofield, 1994). Moreover, in wt MPCs, cyclin D (CycD) expression is maintained due to the mitogenic effect of bFGF (Fig. 3B). By contrast, *Sgca*-null MPCs appeared to be insensitive to bFGF treatment and their proliferation curve was essentially the same with or without bFGF (Fig. 3A, compare black and gray lines). Indeed, CycD expression was barely detectable in bFGF-treated *Sgca*-null MPCs (Fig. 3B). By contrast, HGF treatment induced proliferation in wt MPCs and in both dystrophic MPCs, but no substantial differences existed at any of the time points analyzed (Fig. 3A, dashed lines). Furthermore, HGF-induced CycD expression was comparable in wt and *Sgca*-null MPCs (Fig. 3B).

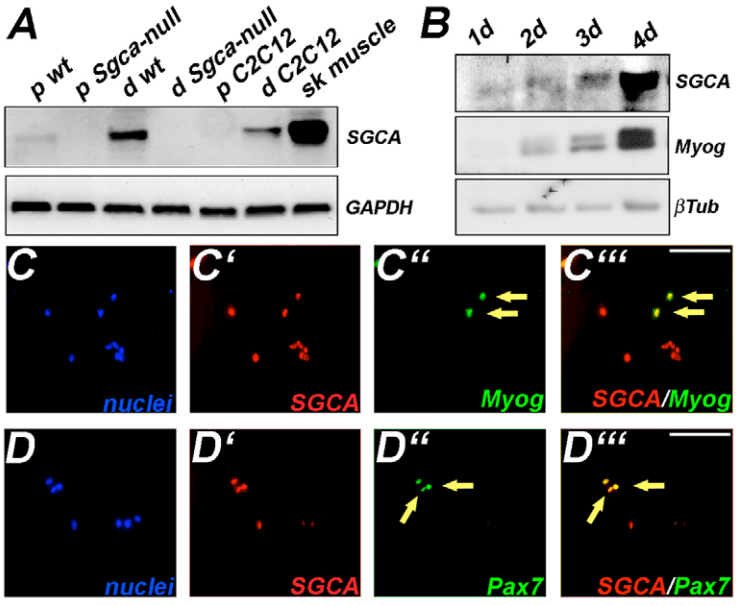

Fig. 2. Expression pattern of SGCA in MPCs. (**A**) Western blot analysis showing SGCA expression in C2C12, wt or *Sgca*-null mouse MPCS in proliferating (p) or differentiating (d) conditions. Skeletal muscle tissue extract (sk muscle) was used as positive control. *n*=3. GAPDH was used as an internal control. (**B**) Western blot (WB) analysis of SGCA and myogenin (Myog) expression in differentiating wt MPCs. *n*=3. β-tubulin (βTub) was used as internal control. (**C-C‴**) Immunofluorescence staining for SGCA (red in C′) and myogenin (green in C″) expression during early stages of differentiation in wt MPCs (day 1 after starvation). Yellow arrows indicate double-positive cells. *n*=4. (**D-D‴**) Representative images of wt MPCs co-expressing SGCA (red in D′) and PAX7 (green in D″). Yellow arrows indicate PAX7^{+}/SGCA^{+} wt MPCs. Scale bars: 100 μm.

DEVELOPMENT

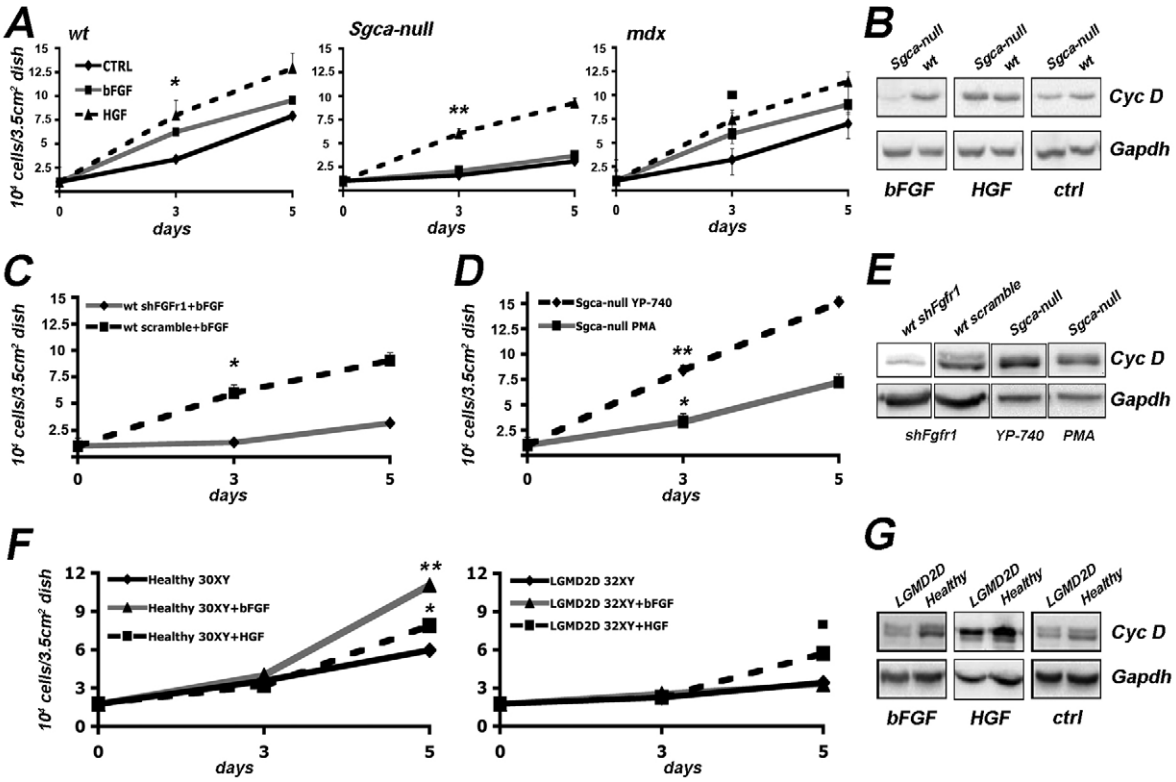

Fig. 3. Proliferative ability following cytokine treatment. (**A**) Total number of cells per clone from wt, *Sgca*-null and *mdx* mouse MPCs grown for 5 days in conditioned media containing bFGF (gray lines) or HGF (dashed lines). CTRL, growth curves of MPCs in non-conditioned media (black lines). n=5; *, P<0.01 for CTRL versus bFGF; **, P<0.01 for CTRL versus HGF; square, P<0.01 CTRL versus bFGF. Error bars indicate s.e.m. (**B**) WB for CycD expression in wt and *Sgca*-null MPCs stimulated with bFGF or HGF. ctrl, MPCs grown in non-conditioned media. GAPDH was used as an internal control. (**C**) Growth curves of wt MPC clones infected with shFGFR1 (gray line) or with scramble control shRNA (black dashed line) stimulated with bFGF. The shFGFR1 wt MPC curve strongly overlaps with that of *Sgca*-null MPCs grown with or without bFGF (compare gray line with *Sgca*-null gray line in A). n=3; *, P<0.01 for shFGFR1 versus scramble. (**D**) Growth curves of *Sgca*-null MPCs treated with YP-740 (black dashed line) or PMA (gray line). n=3; *, P<0.05 for *Sgca* null + bFGF versus PMA; **, P<0.01 for *Sgca* null + bFGF versus YP-740. (**E**) WB analysis for CycD expression in wt MPCs infected with shFGFR1 (lane 1) or with scramble (lane 2), and *Sgca* null treated with YP-740 (lane 3) or PMA (lane 4). n=3. (**F**) Human myoblasts isolated from healthy (30XY, left graph) or LGMD2D (32XY, right graph) patients were stimulated with bFGF (gray lines) or HGF (dashed lines) and the total number of cells was counted (n=5). Black lines, control growth curves of myoblasts in non-conditioned media. n=2 patient biopsies for LGMD2D and healthy myoblasts, respectively. *, P<0.05 for healthy control versus bFGF; **P<0.05 for healthy bFGF versus HGF; square, P<0.001 for LGMD2D bFGF versus HGF using two-way ANOVA test. (**G**) WB analysis for CycD expression in human myoblasts treated with bFGF and HGF. ctrl, human myoblasts grown in non-conditioned media. n=3.

To provide a further link between the absence of *Sgca* expression and bFGF signaling, loss-of-function experiments were performed after FGFR1 knockdown in wt MPC clones using a short hairpin (sh) RNA strategy. Silencing was very effective, as demonstrated by RT-PCR and western blot (WB) analysis of shFGFR1-infected wt MPCs (see Fig. S2C,D in the supplementary material). When treated with bFGF, shFGFR1 wt clones proliferated at a slower rate than scramble-infected control cells (Fig. 3C). The proliferation curve of the shFGFR1 wt clones matched that of the bFGF-treated *Sgca*-null clones (compare gray lines in Fig. 3A and 3C) and expression of CycD (Fig. 3E, lane wt + shFGFR1) and phosphorylated (p) ERK1/2 (also known as MAPK3/1) (see Fig. S3C in the supplementary material) was barely detectable.

Using YP-740 (Derossi et al., 1998) and PMA (Weiss et al., 1994) stimulation, we determined that downstream activation of the bFGF pathway in *Sgca*-null MPCs restores the proliferative rate to levels comparable to wt MPCs, as demonstrated by growth curves (Fig. 3D), CycD (Fig. 3E, lanes *Sgca* null + YP-740 and *Sgca* null + PMA) and pErk1/2 (see Fig. S3C in the supplementary material) expression analysis. A defective bFGF response is also present in humans, with patient-derived bFGF-treated LGMD2D myoblasts showing impaired proliferation compared with their healthy counterparts (Fig. 3F, gray lines). However, HGF treatment led to an increase in the total cell number of both healthy and LGMD2D-derived myoblasts (Fig. 3F, dashed lines). CycD expression analysis of human myoblasts revealed higher levels in healthy myoblasts treated with both bFGF and HGF, whereas LGMD2D-derived myoblasts responded to HGF stimulation only (Fig. 3G). Importantly, WB analysis of pERK1/2 confirmed the impairment of proliferation in *Sgca*-null myogenic cells during bFGF stimulation (see Fig. S3A,B,D in the supplementary material). Additionally, a strong decrease (by 75%) in phosphohistone H3 (pHH3)/MYF5 immunoreactivity in *Sgca*-null MPCs further reinforces the idea that a bFGF-associated impairment in proliferation is present (see Fig. S4A-C in the supplementary material).

It has been reported that the absence of SGCA can alter integrin-dependent adhesion and motility pathways, causing enhanced apoptosis (Allikian et al., 2004; Anastasi et al., 2004; Yoshida et al., 1998). To test this possibility, active caspase 9 (Casp9) levels

were measured in wt and *Sgca*-null MPCs cultured both with and without bFGF or HGF (see Fig. S4D in the supplementary material). Only a modest increase (15%) in Casp9 levels was observed in *Sgca*-null MPCs cultured in the presence of bFGF, making it unlikely that enhanced apoptosis is the main cause for the reduced number of cells observed in *Sgca*-null MPCs. Altogether, these data confirm that the impairment of proliferation in *Sgca*-null MPCs is due to a defective bFGF-FGF receptor axis.

SGCA and FGFR1 associate as a complex

The data reported above suggest a possible link between *Sgca* and bFGF-driven MPC proliferation. To prove this hypothesis, we characterized the expression levels of FGFR1 and FGFR4, which are involved during the myogenic program in vitro and in vivo (Kastner et al., 2000), in wt and *Sgca*-null MPCs. Interestingly, we found that *Sgca*-null MPCs upregulated both *Fgfr1* and *Fgfr4* at the mRNA level in proliferating medium, as compared with their wt counterparts, possibly as a compensatory mechanism (Fig. 4A). These data are consistent with gene expression profiling studies on tibialis anterior muscle from *Sgca*-null mice (Biressi et al., 2007), which show marked upregulation of *Fgfr1* mRNA (see Fig. S5A in the supplementary material).

FGFR1 is normally upregulated during the early differentiation stage of C2C12 cells (see Fig. S5B in the supplementary material). WB analysis revealed similar levels of FGFR1 expression in wt and *Sgca*-null MPCs (Fig. 4B). Similarly, wt and *Sgca*-null MPCs did not show any substantial differences in the expression levels or cellular localization of FGFR4 (see Fig. S5C,D in the supplementary material). These results provide evidence that the proliferative defect of *Sgca*-null MPCs is not a secondary effect of an enhanced FGFR4-dependent spontaneous differentiation.

During proliferation, FGFR1 localized on the cell membrane together with SGCA only in wt MPCs (Fig. 4D,D′), whereas in *Sgca*-null MPCs FGFR1 expression was mainly confined to the nucleus (Fig. 4C,C′) (Kilkenny and Hill, 1996; Myers et al., 2003; Peng et al., 2002). For this reason, we analyzed the subcellular distribution of FGFR1 and SGCA in wt MPCs. Immunohistochemical staining revealed partial colocalization of FGFR1 and SGCA in small, rounded cells, which are likely to be proliferating or early differentiating MPCs (Fig. 4E″, white arrow). Confocal analysis of MPCs at day 1 of differentiation confirmed partial colocalization of the two proteins at the plasma membrane (Fig. 4F″, white arrows). At late stages of differentiation, when myotubes are formed, FGFR1 no longer colocalized with SGCA and was mainly restricted to the nucleus (Fig. 4G″), as previously reported (Myers et al., 2003). To support the claim that FGFR1 and SGCA colocalize on the cell membrane, we assessed the amount of FGFR1 on the cell membrane in wt and *Sgca*-null MPCs by surface protein biotinylation analysis (Fig. 4H). Again, FGFR1 localized on the cell surface only in wt and not in *Sgca*-null MPCs, providing direct evidence that SGCA is required for proper localization of the receptor. Therefore, FGFR1 mislocalization cannot be attributed to the altered expression of heparan sulfate proteoglycans (HSPGs) (Filla et al., 1998; Steinfeld et al., 1996), as demonstrated by WB analysis for syndecan 1 in wt and *Sgca*-null MPCs (Fig. 4B). Taken together, these results suggest that an interaction exists between bFGF signaling and SGCA during MPC proliferation but not after differentiation.

We investigated a possible interaction between SGCA and FGFR1 by immunoprecipitation and WB analysis in non-myogenic and myogenic cells. Human 293T cells expressing *Sgca* and *Fgfr1* under the control of a CMV promoter were subjected to immunoprecipitation analysis. Proteins were resolved from cell lysates using SGCA antibodies as bait and then immunoblotted with FGFR1 antibodies (Fig. 4I). Co-immunoprecipitation experiments on double-transfected 293T cells revealed that SGCA effectively binds FGFR1 (Fig. 4I). The absence of SGCA signal in immunoprecipitates of single-transfected 293T cells (Fig. 4I) highlight the specificity of the interaction. SGCA polyclonal antibodies were also able to co-immunoprecipitate SGCA-FGFR1 complexes in wt skeletal muscle and MPC cultures (lanes 1d, 3d and wt in Fig. 4J), confirming the above results. Moreover, cardiotoxin-induced muscle damage and regeneration augmented the amount of SGCA-FGFR1 complexes detected (lane wt + ctx in Fig. 4J). Thus, SGCA might regulate MPC proliferation via the formation of a complex with FGFR1, rather than playing a structural role as it does after differentiation.

In vivo transplantation of MPCs

To address the possible role of *Sgca* in regulating the self-renewal and myogenic potential of MPCs, wt and dystrophic MPCs were transplanted into an *Sgca*-null recipient. We isolated GFP$^+$ MPCs from wt and *Sgca*-null mice backcrossed with human phosphoglycerate kinase (hPGK)-GFP transgenic animals. Before injection, MPC purity was evaluated by double staining for GFP and MYOD (Fig. 5A-B′) and found to be ~70% for both *Sgca*-null and wt cells (Fig. 5C). The extent of engraftment was evaluated by measuring *GFP* mRNA expression in the injected muscles at different time points. Direct comparison of GFP expression from wt and *Sgca*-null MPCs revealed a profound impairment of engraftment of dystrophic MPCs (Fig. 5D). Wt MPC transplantation resulted in a modest but progressive increase in GFP expression. Conversely, the GFP expression level was initially similar in mice injected with dystrophic MPCs but decreased rapidly to become barely detectable 6 days after injection.

To test whether the engraftment impairment of dystrophic MPCs was due to poor survival, we analyzed apoptosis of donor cells in vivo. MPCs isolated from wt and *Sgca*-null mice were transduced with pLenti-CMV/NLS-nlacZ, a lentiviral vector that expresses a nuclear β-galactosidase (β-gal) reporter. Following lentiviral infection, β-gal$^+$ MPCs were transplanted into the tibialis anterior of juvenile *Sgca*-null mice and apoptotic donor cells were identified by β-gal$^+$/TUNEL$^+$ nuclei. An increase of apoptotic events (more than 2.5-fold higher after 3 days, both in resident and donor cells) was observed in dystrophic mice, reflecting a survival defect in resident *Sgca*-null MPCs (Fig. 5E). Therefore, at day 3 after injection, the apoptotic rate of transplanted cells (the total number of cells that were β-gal$^+$/TUNEL$^+$) was 3-fold higher in dystrophic MPCs than in their wt counterparts (Fig. 5F). At day 10 after injection, when apoptotic events were almost completed, there was no longer any significant difference in the apoptotic rate between wt and dystrophic MPCs (Fig. 5E,F). These data show that SGCA deficiency interferes functionally with the biological properties of MPCs, which become more susceptible to apoptosis and fail to properly colonize skeletal muscle.

Genetic correction of *Sgca*-null MPCs leads to functional rescue

To understand to what extent proliferation defects and increased cell mortality can be attributed to *Sgca* deficiency, genetic correction of dystrophic MPCs was performed. We used a lentiviral vector carrying the murine coding sequence of *Sgca* under the

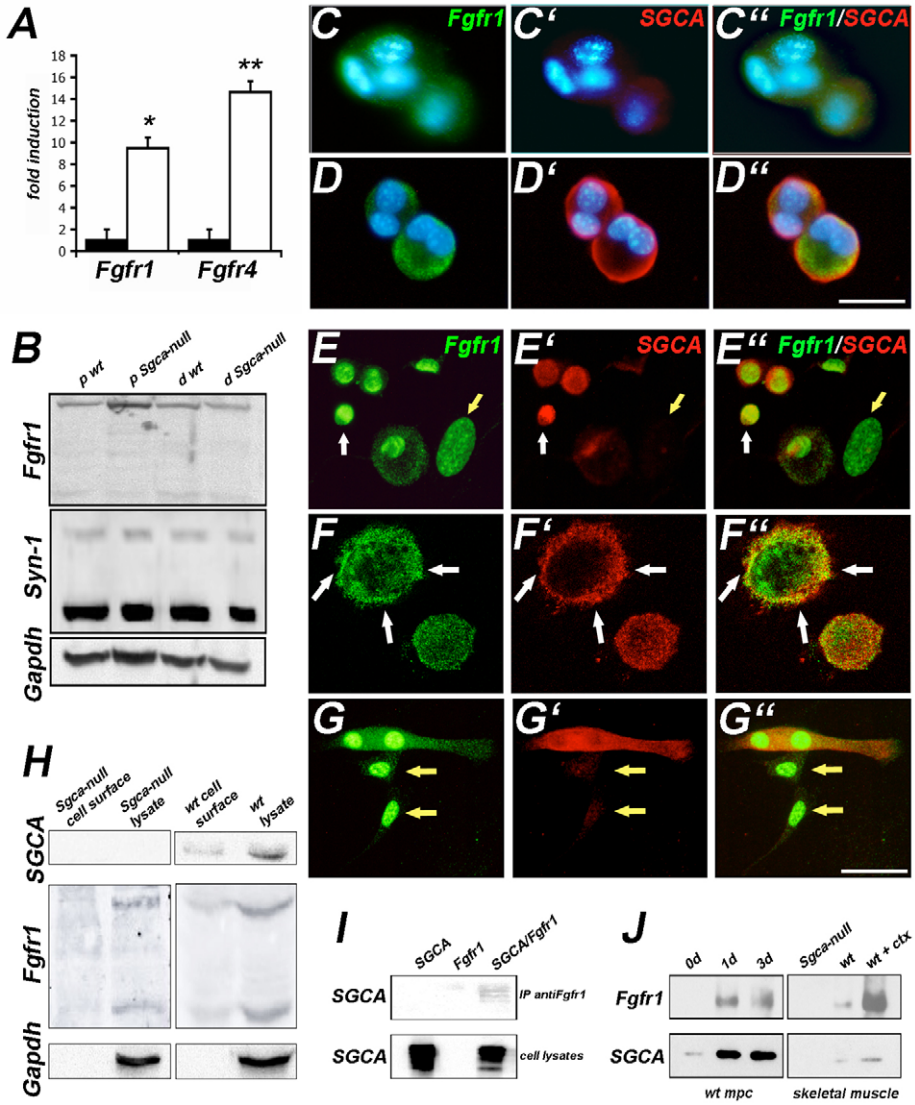

Fig. 4. SGCA directly cooperates with FGFR1. (**A**) qPCR for *Fgfr1* and *Fgfr4* in proliferating *Sgca*-null (white) and wt (black) MPCs. *n*=5; *, *P*<0.01 and **, *P*<0.01 for *Sgca* null versus wt. Error bars indicate s.e.m. (**B**) WB analysis for FGFR1 and syndecan 1 (Syn-1) expression in wt and *Sgca*-null MPCs in proliferating (p) and differentiating (d) conditions. *n*=3. (**C-D″**) Immunofluorescence staining for FGFR1 (green) and SGCA (red) expression in early differentiating MPCs (day 1 after starvation) showing a diverse cellular localization of FGFR1 in *Sgca*-null (C″) and wt (D″) MPCs. SGCA signal in D′ was slightly overexposed to highlight cell membrane borders. *n*=3. (**E-E″**) Immunofluorescence staining for FGFR1 (E, green) and SGCA (E′, red) showed protein colocalization in wt MPCs at an early step of differentiation (day 1 to 2) (E″, white arrows). Such colocalization was not observed in fibroblasts, which were found to be exclusively positive for FGFR1 (E″, yellow arrow). *n*=3. (**F-F″**) Confocal images of early differentiating MPCs (day 1) representing areas of partial colocalization (F″, white arrows) of FGFR1 (green in F) with SGCA (red in F′). *n*=3. (**G-G″**) A newly formed myotube and fibroblasts (G″, yellow arrows) show no colocalization of FGFR1 (green in G) and SGCA (red in G′) signal. *n*=3. (**H**) Surface protein biotinylation assay showing that FGFR1 is expressed both by wt (wt lysate) and *Sgca*-null (*Sgca*-null lysate) MPCs but can localize on the cell membrane together with SGCA only in wt MPCs (wt cell surface). No FGFR1 signal was detected in the surface protein fraction of *Sgca*-null MPCs (*Sgca*-null cell surface). β-tubulin was used as an internal control for the cell lysate fractions. *n*=3. (**I**) Immunoprecipitation analysis in 293T cells co-expressing SGCA and FGFR1, revealing an interaction of SGCA with FGFR1 (top, SGCA/Fgfr1). No signal was detected in 293T cells transfected only with vectors expressing *Sgca* (top, SGCA) or *Fgfr1* (top, Fgfr1). *n*=3. (**J**) WB analysis of wt MPCs and muscle tissue extracts from wt and *Sgca*-null mice immunoprecipitated with SGCA polyclonal antibodies and detected with FGFR1 (top) and SGCA (bottom) monoclonal antibodies. FGFR1 co-immunoprecipitates with SGCA in samples derived from early differentiating wt MPCs (1d and 3d), skeletal muscle tissue extract (wt) and muscle crushed with cardiotoxin (wt + ctx). No signal was obtained from proliferating wt MPCs (0d) or *Sgca*-null skeletal muscle. *n*=3. Scale bars: 30 μm in C-D″; 50 μm in E-G″.

control of a CMV promoter and fused it in frame with a synthetic V5 epitope to further discriminate protein localization. We obtained 95% transduction efficiency after one round of infection at a multiplicity of infection of 10 (data not shown). Genetic correction led to an increase in the number of cells per *Sgca*-null MPC clone as compared with non-corrected MPCs (Fig. 6A-C). Moreover, when the myogenic potential of corrected MPCs was analyzed under differentiating conditions, cells formed large multinucleated

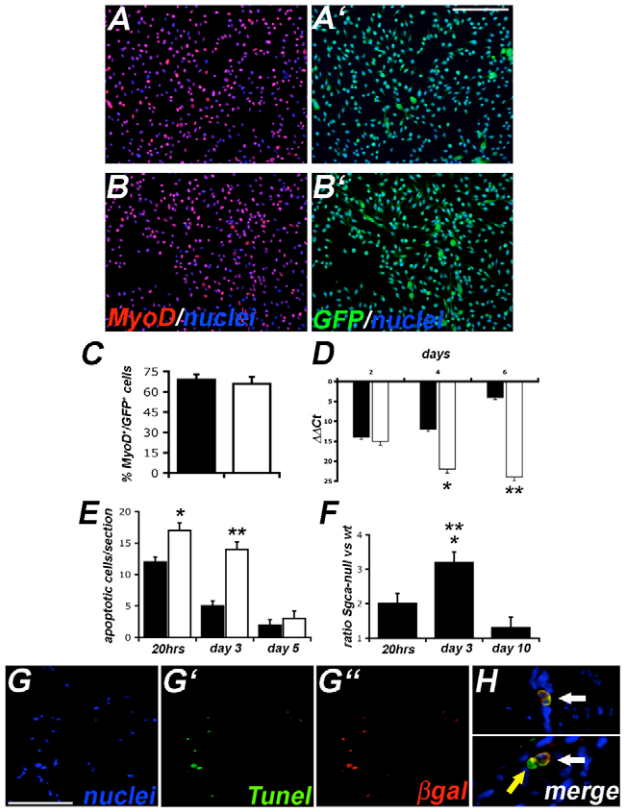

Fig. 5. In vivo transplantation of dystrophic MPCs failed to reconstitute the myogenic compartment. (**A-B′**) MPCs isolated from wt (A,A′) and *Sgca*-null (B,B′) mice backcrossed with GFP transgenic mice. MPC purity was evaluated by double staining for MYOD (red in A,B) and GFP (green in A′,B′) expression. (**C**) Percentage MYOD$^+$/GFP$^+$ cells from wt (black) and *Sgca*-null (white) mice. n=200 clones. (**D**) qPCR for *GFP* expression at 2, 4 and 6 days following intramuscular injections of wt (black) and *Sgca*-null (white) GFP$^+$ MPCs into the tibialis anterior of *Sgca*-null juvenile mice. Three mice were injected per time point for a total of nine mice per group. n=18 mice; *, P<0.01 and **, P<0.01 for *Sgca* null versus wt. (**E**) *nlacZ*$^+$ MPCs (5×10^5) were injected into the tibialis anterior of juvenile 3-week-old *Sgca*-null mice. Global cell death rate was calculated by counting TUNEL$^+$ cells at three different time points (20 hours, 3 and 10 days). Three mice were injected per time point for a total of nine mice per group. n=18; *, P<0.01 and **, P<0.01 for *Sgca*-null versus wt. (**F**) Double staining for β-gal and TUNEL revealed the apoptotic rate of injected MPCs. Approximately 100 muscle sections were analyzed at each time point. n<100; *, P<0.01 for day 3 versus day 10; **, P<0.01 for day 3 versus 20 hours. Error bars (C-F) indicate s.e.m. (**G-G″**) Representative images of TUNEL$^+$ *Sgca*-null donor cells. At day 3 after injection, massive cell death of dystrophic MPCs was observed. Apoptotic donor cells are β-gal$^+$ (G″, red) and TUNEL$^+$ (G′, green). (**H**) High-magnification images of donor MPCs (white arrows) following transplantation. In the bottom panel, a TUNEL$^+$/β-gal$^+$ *Sgca*-null MPC is situated close to an endogenous apoptotic cell (TUNEL$^+$/β-gal$^-$, yellow arrow). Scale bars: 100 μm.

myotubes (Fig. 6D,D′) with the number of nuclei per myotube comparable to that in wt (Fig. 6E). In addition to the rescue of proliferation, genetic correction restores the SGCA-FGFR1 interaction, as pull-down experiments in corrected *Sgca*-null MPCs detected the presence of FGFR1 in protein extracts precipitated with an anti-SGCA antibody (Fig. 6F).

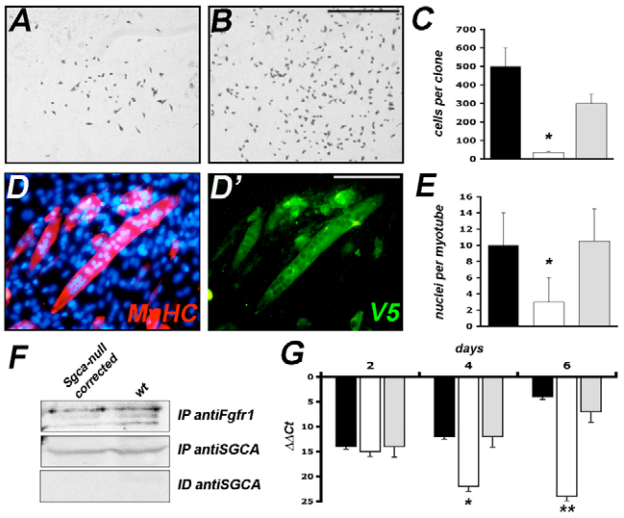

Fig. 6. Genetic correction restores the myogenic potential of *Sgca*-null MPCs. (**A**,**B**) Phase contrast images of single clones from corrected (B) and non-corrected (A) *Sgca*-null MPCs. (**C**) Number of cells per clone of corrected (gray) and non-corrected (white) *Sgca*-null MPCs. Black bars indicate wt MPCs. n=5; *, P<0.01 for corrected versus non-corrected MPCs. (**D**,**D′**) MyHC (red) and V5 (green) staining of *Sgca*-null corrected cells. n=5. (**E**) Number of nuclei per myotube of corrected (gray) and non-corrected (white) *Sgca*-null MPCs. Black bars indicate wt MPCs. n=5 experiments performed in triplicate; *, P<0.01 for corrected versus non-corrected MPCs. (**F**) WB analysis of protein extracts from corrected *Sgca*-null and wt MPCs immunoprecipitated with SGCA polyclonal antibodies and detected with FGFR1 (top) and SGCA (middle) monoclonal antibodies. No SGCA signal was obtained from the immunodepleted (ID) fraction (bottom). n=3. (**G**) qPCR for *GFP* expression at 2, 4 and 6 days following intramuscular injections of wt (black), corrected *Sgca*-null (gray) and non-corrected *Sgca*-null (white) GFP$^+$ MPCs into the tibialis anterior of *Sgca*-null juvenile mice. Three mice were injected per time point for a total of nine mice per group. n=18 mice; *, P<0.01 and **, P<0.01 for corrected versus non-corrected MPCs. Error bars (C,E,G) indicate s.e.m. Scale bars: 200 μm in A,B; 100 μm in D,D′.

Corrected *Sgca*-null GFP$^+$ MPCs were injected into dystrophic mice to further investigate their capacity for functional rescue. In vivo engraftment of *Sgca*-null MPCs was restored, as demonstrated by high levels of GFP expression in injected muscles at all time points analyzed (Fig. 6G).

Altogether, these data support the hypothesis that lack of *Sgca* expression affects MPC proliferation as well as cell survival by interfering with bFGF signaling.

DISCUSSION

Satellite cells are quiescent mononucleated cells, located between the basal lamina and sarcolemma of adult skeletal muscle (Gnocchi et al., 2009; Mauro, 1961; Zammit et al., 2006). They contribute to postnatal growth by supplying myonuclei to the growing muscle fibers and become quiescent at the end of postnatal growth (Le Grand and Rudnicki, 2007). However, upon injury to the tissue, satellite cells become activated and proliferate as MPCs. MPCs function to repair or replace damaged fibers (Cassano et al., 2009; Collins et al., 2005) and then part of the cell population returns to quiescence in order to replenish the satellite cell pool (Zammit et al., 2004). Therefore, satellite cells are considered the unipotent adult stem cells of skeletal muscle (Zammit et al., 2006).

Satellite cells are the most relevant to muscle repair because of their abundance, location and robust myogenic commitment (Cossu and Biressi, 2005). However, the development of cell therapies based upon satellite cell transplantation has been hampered by poor engraftment, poor ability to migrate inside the tissue and an inability to cross the endothelial barrier when injected into the vasculature (Cossu and Sampaolesi, 2007; Sampaolesi et al., 2003). In previous work, we observed that systemic delivery of mesoderm progenitors, termed mesoangioblasts, rescued the dystrophic phenotype of *Sgca*-null mice. The success of this approach was mainly due to widespread distribution of donor cells through the capillary network. As in other cases of successful engraftment (Aiuti et al., 2002), we questioned whether mesoangioblast transplantation into *Sgca*-null mice had been favored as a result of poor competition with resident satellite cells. In other cases of cell transplantation in *mdx* dystrophic mice (Montanaro et al., 2003; Torrente et al., 2004), although engraftment and dystrophin reconstitution have been documented, the extent of recovery was less successful than for the *Sgca*-null mice. This might depend upon the better engraftment potential of mesoangioblasts in comparison with side population (SP) or AC133 cells, or, alternatively, be influenced by a different microenvironment in the two types of dystrophic mice. Differences in transplantation efficiency might concern the level of inflammatory cell infiltration, the deposition of fibrous tissue, as well as the biological features of resident myogenic progenitors. Therefore, we focused on the satellite cells of *Sgca*-null mice, assuming that a defect in these cells might result in reduced competition with donor cells, thus explaining the extensive engraftment and phenotypic rescue elicited by mesoangioblast transplantation in the *Sgca*-null mouse.

In this work, we have studied the role of SGCA in satellite cell proliferation and differentiation. In the late 1980s, DiMario and Strohman reported that when satellite cells cultured from *mdx* and control mouse hindlimb muscles are stimulated with bFGF, they proliferate and fuse to form muscle fibers within 4 to 5 days (DiMario and Strohman, 1988). We found that *Sgca*-null satellite cells show reduced proliferation in comparison with their wt or *mdx* counterparts owing to reduced sensitivity to bFGF, a major mitogen for these cells. The proliferative defect of *Sgca*-null myogenic precursors was confirmed by both clonogenic assays and by single fiber analysis. Importantly, this effect was specific for bFGF, as proliferation in response to HGF, another mitogen for satellite cells (Gal-Levi et al., 1998), was unaltered.

In order to elicit any effect on proliferating MPCs, SGCA should be expressed at detectable levels during proliferation, when dystrophin and most of the other associated proteins are not yet expressed. Indeed, we observed expression of SGCA at the early stages of satellite cell activation, when we detected $PAX7^{+}/SGCA^{+}$ MPCs. At these stages, SGCA colocalizes with FGFR1 and a lack of SGCA expression in MPCs alters the localization of the receptor, which leads to intracellular accumulation of FGFR1. Although modest amounts of SGCA may be sufficient to help FGFR1 localization on the cell membrane, higher levels are needed for SGCA to play its structural role as a DGC member. This fact might well explain the upregulation of SGCA expression during differentiation. Our co-immunoprecipitation studies confirmed the formation of a complex between SGCA and FGFR1 in MPCs, but also confirmed complex formation in a non-myogenic cell system in which both proteins were overexpressed. Thus, under normal conditions, SGCA positively modulates FGF signaling by forming stable complexes with FGFR1.

FGFR1 is present in both myogenic and non-myogenic cells in adult skeletal muscle (Kastner et al., 2000) and muscle development and homeostasis are severely affected when FGFR1 is absent (Marics et al., 2002). Previous studies put forth the hypothesis that FGFR4 expression patterns correlate with the growth-differentiation transition of satellite cells, whereas FGFR1 is mainly involved in maintaining the proliferative state of MPCs (Itoh et al., 1996; Marics et al., 2002; Olwin et al., 1994; Weinstein et al., 1998). The observation that the expression levels and cellular localization of FGFR4 were unaffected in *Sgca*-null as compared with wt MPCs rules out the possibility that the proliferation impairment in *Sgca*-null MPCs is a consequence of enhanced FGFR4-dependent differentiation. Impaired proliferation was reverted by transduction with lentiviral vectors carrying the *Sgca* gene, confirming a direct role of *Sgca* in MPC proliferation impairment.

MPCs isolated from *Sgca*-null mice failed to properly colonize the regenerating muscle, whereas wt cells engrafted efficiently and survived in vivo. Interestingly, an association of SGCA with integrins has been reported (Allikian et al., 2004; Anastasi et al., 2004; Yoshida et al., 1998), and thus the absence of SGCA might also contribute to impaired migration through inadequate integrin-dependent adhesion and motility. This might also explain, at in least in part, the enhanced apoptosis observed in *Sgca*-null MPCs in vitro and in vivo.

The regulation of the cell cycle and cell death are often coupled and a fine balance between these processes is required for many biological processes, such as tissue development and homeostasis and regeneration (Gil-Gomez et al., 1998). Here, we present evidence for a synergistic effect between defective bFGF signaling and enhanced apoptosis resulting in a functional defect of *Sgca*-null MPCs.

Two main features distinguish muscular dystrophy in *Sgca*-null versus *mdx* mice: the early onset of the disease and the severity of the pathology. In *mdx* mice, the pathology is mild after a degeneration-regeneration crisis at 3-4 weeks of age (McArdle et al., 1995), whereas the persistence of degeneration in *Sgca*-null mice results in a more severe pathology.

In our initial attempt at cell therapy for muscular dystrophy, we selected *Sgca*-null mice for the reasons outlined above. The results we obtained were better than those obtained with *mdx*, but we did not know at that time that the success in engraftment was due, at least in part, to the proliferation impairment of *Sgca*-null satellite cells. In line with this observation, the phenotype of *mdx* mice is dramatically worsened if proliferation of satellite cells is hampered by deletion of the telomerase gene (Sacco et al., 2010) or when the endogenous progenitors are exhausted with long-term serial and intense exercise, with consequent enhanced mesoangioblast engraftment (Tedesco et al., 2011). Interestingly, the same proliferation defect is observed in human MPCs from LGMD2D patients, whose dystrophy, however, remains milder than DMD. This could be explained by the fact that human cells show a reduced proliferative potency compared with those of mice, and that other factors, such as the residual expression of dystrophin (Klinge et al., 2008; Vainzof et al., 2000), might act at the level of fiber stability rather than in the regeneration process. The phenotypic difference observed between LGMD2D and *Sgca*-null mice, together with the large variability in the severity of the human disease, might also reflect the mutation type of the *SGCA* gene together with species-specific compensatory and regulatory mechanisms (Kobuke et al., 2008).

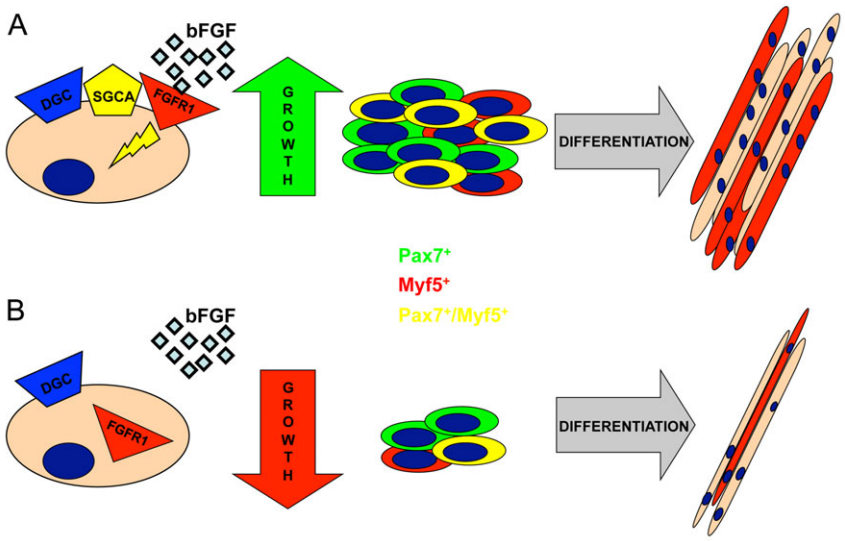

Fig. 7. SGCA/bFGF signaling during proliferation of MPCs. (**A**) wt MPCs respond to bFGF by augmenting their proliferation and consequently increasing the myogenic-committed pool. SGCA plays an important role during the proliferation and early differentiation phases in MPCs by cooperating with FGFR1 and thus stabilizing the complex on the cell membrane. (**B**) In the absence of *Sgca* expression, FGFR1 is mainly localized in the nucleus and *Sgca*-null MPCs lack sensitivity to bFGF stimulation. Under these conditions, *Sgca*-null MPCs fail to activate a proliferative input, having instead as a final readout an impairment in self-renewal and homing.

SGCA is crucial for postnatal myogenesis. It forms a complex with dystrophin in differentiated muscle and participates in bFGF and integrin signaling as part of a program that regulates satellite cell proliferation and survival. bFGF stimulates proliferation and prevents the precocious differentiation of satellite cell-derived MPCs (Lapidos et al., 2004; Sheehan and Allen, 1999). The SGCA-FGFR1 interaction is necessary for this proliferative signaling. When the myogenic pattern is upregulated, as satellite cell progeny differentiate, the SGCA-FGFR1 interaction ceases and the SGCA acquires its definitive role in the membrane dystrophin complex (Fig. 7).

Acknowledgements
We thank Gianpaolo Papaccio for critical discussion of the manuscript; K. P. Campbell for providing *Sgca*-null mice; Laura Perani, Rossana Tonlorenzi and Rudi Micheletti for technical assistance; Christina Vochten for professional secretarial service; Paolo Luban for a kind donation; Dr Shea Carter for manuscript editing; and Dr Maurizio Moggio (Bank of DNA, Cell Lines and Nerve-Muscle-Cardiac Tissues/Telethon Genetic BioBank Network, Ospedale Maggiore Policlinico Mangiagalli e Regina Elena, Milan, Italy) for providing the LGMD2D sample.

Funding
This work was supported in part by FWO-Odysseus Program Grant No. G.0907.08; Research Council of the University of Leuven, Grant No. OT/09/053 and EME-C2161-GOA/11/012; Wicka Charity Funds, USA, Grant No. zkb8720; the Italian Ministry of University and Scientific Research Grant No. 2005067555_003, PRIN 2006-08, CARIPLO 2007.5639 and 2005.2008; EC FP7 CARE-MI No. 242038; and Optistem No. 223098.

Competing interests statement
The authors declare no competing financial interests.

Supplementary material
Supplementary material for this article is available at
http://dev.biologists.org/lookup/suppl/doi:10.1242/dev.070706/-/DC1

References

Aiuti, A., Slavin, S., Aker, M., Ficara, F., Deola, S., Mortellaro, A., Morecki, S., Andolfi, G., Tabucchi, A., Carlucci, F. et al. (2002). Correction of ADA-SCID by stem cell gene therapy combined with nonmyeloablative conditioning. *Science* **296**, 2410-2413.

Alameddine, H. S., Dehaupas, M. and Fardeau, M. (1989). Regeneration of skeletal muscle fibers from autologous satellite cells multiplied in vitro. An experimental model for testing cultured cell myogenicity. *Muscle Nerve* **12**, 544-555.

Allen, R. E. and Boxhorn, L. K. (1989). Regulation of skeletal muscle satellite cell proliferation and differentiation by transforming growth factor-beta, insulin-like growth factor I, and fibroblast growth factor. *J. Cell. Physiol.* **138**, 311-315.

Allikian, M. J., Hack, A. A., Mewborn, S., Mayer, U. and McNally, E. M. (2004). Genetic compensation for sarcoglycan loss by integrin alpha7beta1 in muscle. *J. Cell Sci.* **117**, 3821-3830.

Anastasi, G., Cutroneo, G., Rizzo, G., Arco, A., Santoro, G., Bramanti, P., Vitetta, A. G., Pisani, A., Trimarchi, F. and Favaloro, A. (2004). Sarcoglycan and integrin localization in normal human skeletal muscle: a confocal laser scanning microscope study. *Eur. J. Histochem.* **48**, 245-252.

Biressi, S., Tagliafico, E., Lamorte, G., Monteverde, S., Tenedini, E., Roncaglia, E., Ferrari, S., Cusella-De Angelis, M. G., Tajbakhsh, S. and Cossu, G. (2007). Intrinsic phenotypic diversity of embryonic and fetal myoblasts is revealed by genome-wide gene expression analysis on purified cells. *Dev. Biol.* **304**, 633-651.

Blau, H. M., Webster, C. and Pavlath, G. K. (1983). Defective myoblasts identified in Duchenne muscular dystrophy. *Proc. Natl. Acad. Sci. USA* **80**, 4856-4860.

Cassano, M., Quattrocelli, M., Crippa, S., Perini, I., Ronzoni, F. and Sampaolesi, M. (2009). Cellular mechanisms and local progenitor activation to regulate skeletal muscle mass. *J. Muscle Res. Cell Motil.* **30**, 243-253.

Collins, C. A., Olsen, I., Zammit, P. S., Heslop, L., Petrie, A., Partridge, T. A. and Morgan, J. E. (2005). Stem cell function, self-renewal, and behavioral heterogeneity of cells from the adult muscle satellite cell niche. *Cell* **122**, 289-301.

Cossu, G. and Biressi, S. (2005). Satellite cells, myoblasts and other occasional myogenic progenitors: possible origin, phenotypic features and role in muscle regeneration. *Semin. Cell Dev. Biol.* **16**, 623-631.

Cossu, G. and Sampaolesi, M. (2007). New therapies for Duchenne muscular dystrophy: challenges, prospects and clinical trials. *Trends Mol. Med.* **13**, 520-526.

Cossu, G., Zani, B., Coletta, M., Bouche, M., Pacifici, M. and Molinaro, M. (1980). In vitro differentiation of satellite cells isolated from normal and dystrophic mammalian muscles. A comparison with embryonic myogenic cells. *Cell Differ.* **9**, 357-368.

Dellavalle, A., Sampaolesi, M., Tonlorenzi, R., Tagliafico, E., Sacchetti, B., Perani, L., Innocenzi, A., Galvez, B. G., Messina, G., Morosetti, R. et al. (2007). Pericytes of human skeletal muscle are myogenic precursors distinct from satellite cells. *Nat. Cell Biol.* **9**, 255-267.

Derossi, D., Williams, E. J., Green, P. J., Dunican, D. J. and Doherty, P. (1998). Stimulation of mitogenesis by a cell-permeable PI 3-kinase binding peptide. *Biochem. Biophys. Res. Commun.* **251**, 148-152.

DiMario, J. and Strohman, R. C. (1988). Satellite cells from dystrophic (mdx) mouse muscle are stimulated by fibroblast growth factor in vitro. *Differentiation* **39**, 42-49.

Duclos, F., Straub, V., Moore, S. A., Venzke, D. P., Hrstka, R. F., Crosbie, R. H., Durbeej, M., Lebakken, C. S., Ettinger, A. J., van der Meulen, J. et al. (1998). Progressive muscular dystrophy in alpha-sarcoglycan-deficient mice. *J. Cell Biol.* **142**, 1461-1471.

Filla, M. S., Dam, P. and Rapraeger, A. C. (1998). The cell surface proteoglycan syndecan-1 mediates fibroblast growth factor-2 binding and activity. *J. Cell. Physiol.* **174**, 310-321.

Fukada, S., Morikawa, D., Yamamoto, Y., Yoshida, T., Sumie, N., Yamaguchi, M., Ito, T., Miyagoe-Suzuki, Y., Takeda, S., Tsujikawa, K. et al. (2010). Genetic background affects properties of satellite cells and mdx phenotypes. *Am. J. Pathol.* **176**, 2414-2424.

Gal-Levi, R., Leshem, Y., Aoki, S., Nakamura, T. and Halevy, O. (1998). Hepatocyte growth factor plays a dual role in regulating skeletal muscle satellite cell proliferation and differentiation. *Biochim. Biophys. Acta* **1402**, 39-51.
Gil-Gomez, G., Berns, A. and Brady, H. J. (1998). A link between cell cycle and cell death: Bax and Bcl-2 modulate Cdk2 activation during thymocyte apoptosis. *EMBO J.* **17**, 7209-7218.
Gnocchi, V. F., White, R. B., Ono, Y., Ellis, J. A. and Zammit, P. S. (2009). Further characterisation of the molecular signature of quiescent and activated mouse muscle satellite cells. *PLoS One* **4**, e5205.
Henry, M. D. and Campbell, K. P. (1996). Dystroglycan: an extracellular matrix receptor linked to the cytoskeleton. *Curr. Opin. Cell Biol.* **8**, 625-631.
Itoh, N., Mima, T. and Mikawa, T. (1996). Loss of fibroblast growth factor receptors is necessary for terminal differentiation of embryonic limb muscle. *Development* **122**, 291-300.
Johnson, S. E. and Allen, R. E. (1995). Activation of skeletal muscle satellite cells and the role of fibroblast growth factor receptors. *Exp. Cell Res.* **219**, 449-453.
Kastner, S., Elias, M. C., Rivera, A. J. and Yablonka-Reuveni, Z. (2000). Gene expression patterns of the fibroblast growth factors and their receptors during myogenesis of rat satellite cells. *J. Histochem. Cytochem.* **48**, 1079-1096.
Kilkenny, D. M. and Hill, D. J. (1996). Perinuclear localization of an intracellular binding protein related to the fibroblast growth factor (FGF) receptor 1 is temporally associated with the nuclear trafficking of FGF-2 in proliferating epiphyseal growth plate chondrocytes. *Endocrinology* **137**, 5078-5089.
Klinge, L., Dekomien, G., Aboumousa, A., Charlton, R., Epplen, J. T., Barresi, R., Bushby, K. and Straub, V. (2008). Sarcoglycanopathies: can muscle immunoanalysis predict the genotype? *Neuromuscul. Disord.* **18**, 934-941.
Kobuke, K., Piccolo, F., Garringer, K. W., Moore, S. A., Sweezer, E., Yang, B. and Campbell, K. P. (2008). A common disease-associated missense mutation in alpha-sarcoglycan fails to cause muscular dystrophy in mice. *Hum. Mol. Genet.* **17**, 1201-1213.
Lapidos, K. A., Kakkar, R. and McNally, E. M. (2004). The dystrophin glycoprotein complex: signaling strength and integrity for the sarcolemma. *Circ. Res.* **94**, 1023-1031.
Le Grand, F. and Rudnicki, M. (2007). Satellite and stem cells in muscle growth and repair. *Development* **134**, 3953-3957.
Lefaucheur, J. P., Pastoret, C. and Sebille, A. (1995). Phenotype of dystrophinopathy in old mdx mice. *Anat. Rec.* **242**, 70-76.
Liu, L. A. and Engvall, E. (1999). Sarcoglycan isoforms in skeletal muscle. *J. Biol. Chem.* **274**, 38171-38176.
Marics, I., Padilla, F., Guillemot, J. F., Scaal, M. and Marcelle, C. (2002). FGFR4 signaling is a necessary step in limb muscle differentiation. *Development* **129**, 4559-4569.
Mauro, A. (1961). Satellite cell of skeletal muscle fibers. *J. Biophys. Biochem. Cytol.* **9**, 493-495.
McArdle, A., Edwards, R. H. and Jackson, M. J. (1995). How does dystrophin deficiency lead to muscle degeneration?-evidence from the mdx mouse. *Neuromuscul. Disord.* **5**, 445-456.
McNally, E. M., Yoshida, M., Mizuno, Y., Ozawa, E. and Kunkel, L. M. (1994). Human adhalin is alternatively spliced and the gene is located on chromosome 17q21. *Proc. Natl. Acad. Sci. USA* **91**, 9690-9694.
Montanaro, F., Liadaki, K., Volinski, J., Flint, A. and Kunkel, L. M. (2003). Skeletal muscle engraftment potential of adult mouse skin side population cells. *Proc. Natl. Acad. Sci. USA* **100**, 9336-9341.
Myers, J. M., Martins, G. G., Ostrowski, J. and Stachowiak, M. K. (2003). Nuclear trafficking of FGFR1: a role for the transmembrane domain. *J. Cell. Biochem.* **88**, 1273-1291.
Olwin, B. B., Arthur, K., Hannon, K., Hein, P., McFall, A., Riley, B., Szebenyi, G., Zhou, Z., Zuber, M. E., Rapraeger, A. C. et al. (1994). Role of FGFs in skeletal muscle and limb development. *Mol. Reprod. Dev.* **39**, 90-101.
Peng, H., Myers, J., Fang, X., Stachowiak, E. K., Maher, P. A., Martins, G. G., Popescu, G., Berezney, R. and Stachowiak, M. K. (2002). Integrative nuclear FGFR1 signaling (INFS) pathway mediates activation of the tyrosine hydroxylase gene by angiotensin II, depolarization and protein kinase C. *J. Neurochem.* **81**, 506-524.
Sacco, A., Mourkioti, F., Tran, R., Choi, J., Llewellyn, M., Kraft, P., Shkreli, M., Delp, S., Pomerantz, J. H., Artandi, S. E. et al. (2010). Short telomeres and stem cell exhaustion model Duchenne muscular dystrophy in mdx/mTR mice. *Cell* **143**, 1059-1071.
Sampaolesi, M., Torrente, Y., Innocenzi, A., Tonlorenzi, R., D'Antona, G., Pellegrino, M. A., Barresi, R., Bresolin, N., De Angelis, M. G., Campbell, K. P. et al. (2003). Cell therapy of alpha-sarcoglycan null dystrophic mice through intra-arterial delivery of mesoangioblasts. *Science* **301**, 487-492.
Sheehan, S. M. and Allen, R. E. (1999). Skeletal muscle satellite cell proliferation in response to members of the fibroblast growth factor family and hepatocyte growth factor. *J. Cell. Physiol.* **181**, 499-506.
Shinin, V., Gayraud-Morel, B., Gomes, D. and Tajbakhsh, S. (2006). Asymmetric division and cosegregation of template DNA strands in adult muscle satellite cells. *Nat. Cell Biol.* **8**, 677-687.
Smith, J. and Schofield, P. N. (1994). The effects of fibroblast growth factors in long-term primary culture of dystrophic (mdx) mouse muscle myoblasts. *Exp. Cell Res.* **210**, 86-93.
Steinfeld, R., Van Den Berghe, H. and David, G. (1996). Stimulation of fibroblast growth factor receptor-1 occupancy and signaling by cell surface-associated syndecans and glypican. *J. Cell Biol.* **133**, 405-416.
Tedesco, F. S., Hoshiya, H., D'Antona, G., Gerli, M. F., Messina, G., Antonini, S., Tonlorenzi, R., Benedetti, S., Berghella, L., Torrente, Y. et al. (2011). Stem cell-mediated transfer of a human artificial chromosome ameliorates muscular dystrophy. *Sci. Transl. Med.* **3**, 96ra78.
Torrente, Y., Belicchi, M., Sampaolesi, M., Pisati, F., Meregalli, M., D'Antona, G., Tonlorenzi, R., Porretti, L., Gavina, M., Mamchaoui, K. et al. (2004). Human circulating AC133(+) stem cells restore dystrophin expression and ameliorate function in dystrophic skeletal muscle. *J. Clin. Invest.* **114**, 182-195.
Vainzof, M., Passos-Bueno, M. R., Canovas, M., Moreira, E. S., Pavanello, R. C., Marie, S. K., Anderson, L. V., Bonnemann, C. G., McNally, E. M., Nigro, V. et al. (1996). The sarcoglycan complex in the six autosomal recessive limb-girdle muscular dystrophies. *Hum. Mol. Genet.* **5**, 1963-1969.
Vainzof, M., Moreira, E. S., Canovas, M., Anderson, L. V., Pavanello, R. C., Passos-Bueno, M. R. and Zatz, M. (2000). Partial alpha-sarcoglycan deficiency with retention of the dystrophin-glycoprotein complex in a LGMD2D family. *Muscle Nerve* **23**, 984-988.
Weinstein, M., Xu, X., Ohyama, K. and Deng, C. X. (1998). FGFR-3 and FGFR-4 function cooperatively to direct alveogenesis in the murine lung. *Development* **125**, 3615-3623.
Weiss, L., Lubin, I., Factorowich, I., Lapidot, Z., Reich, S., Reisner, Y. and Slavin, S. (1994). Effective graft-versus-leukemia effects independent of graft-versus-host disease after T cell-depleted allogeneic bone marrow transplantation in a murine model of B cell leukemia/lymphoma. Role of cell therapy and recombinant IL-2. *J. Immunol.* **153**, 2562-2567.
Yoshida, T., Pan, Y., Hanada, H., Iwata, Y. and Shigekawa, M. (1998). Bidirectional signaling between sarcoglycans and the integrin adhesion system in cultured L6 myocytes. *J. Biol. Chem.* **273**, 1583-1590.
Zammit, P. S., Golding, J. P., Nagata, Y., Hudon, V., Partridge, T. A. and Beauchamp, J. R. (2004). Muscle satellite cells adopt divergent fates: a mechanism for self-renewal? *J. Cell Biol.* **166**, 347-357.
Zammit, P. S., Partridge, T. A. and Yablonka-Reuveni, Z. (2006). The skeletal muscle satellite cell: the stem cell that came in from the cold. *J. Histochem. Cytochem.* **54**, 1177-1191.